NUMERICAL MODELLING OF THE REFLECTION SPECTRUM OF VENUS IN THE VISUAL AND NEAR INFRARED RANGES

E. M. FEIGELSON
Institute of Optics of the Atmosphere, Tomsk, U.S.S.R.
N. L. LUKASHEVICH
Institute of Applied Mathematics, Moscow, U.S.S.R.
and
G. M. KREKOV and G. A. TYTOV
Institute of Optics of the Atmosphere, Tomsk, U.S.S.R.

Abstract. The influence of a dense molecular atmosphere under a cloud layer on spectral albedo of a planet is investigated. The lengths of paths of protons in the clouds are calculated. Experimental spectral transmission functions were used to calculate gas absorption. The results are compared with experimental data.

Our attempts of numerical modelling of the reflection spectrum have, among numerous other attempts, the following particular features:

(a) the influence of the molecular underlayer is investigated,

(b) the absorption in bands of CO_2 gas is taken into account rather completely, together with multiple scattering and absorption by cloud particles.

1. The Spectral Albedo in the Visual Range

Almost the whole optical thickness due to molecular scattering is in the layer $z \leqslant 50$ km. If the lower boundary of the cloud is not below 50 km, it is reasonable to consider a two-layer system: the cloud, and the pure molecular atmosphere below it.

The problem was: given the known optical properties of the molecular layer (the Rayleigh optical thickness, $\tau_{R,\lambda}$; the scattering function, $\gamma_R(\varphi)$; and the single scattering albedo, $\omega = 1$), and for given models of the cloud layer (the size distribution of cloud particles and their refractive index), to find the spectral optical thicknesses of the cloud that reproduce the experimental albedo spectrum.

Two models were considered:

1.1. A cloud layer similar to terrestrial clouds: $r_{\text{mod}} = 10\ \mu$m, having Deirmendjian's scattering function with mean cosine of the scattering angle 0.83. In this case $\tau_\lambda = $ const, and with $\tau_\lambda = 60$ the calculated albedo corresponds to the measured one, as Figure 1 shows. The decrease of the albedo A_λ with wavelength above 0.6 μm is due to to include absorption. The cross on the curve at $\lambda_0 = 0.55\ \mu$m denotes the value of A_{λ_0} with $\omega = 0.998$.

1.2. The second model has $r_{\text{mod}} = 1.1\ \mu$m; $n = 1.44$, as the polarization measurements suggest. In this case the optical thickness of the cloud and the scattering function

Woszczyk and Iwaniszewska (eds.), Exploration of the Planetary System, 185–189. All Rights Reserved

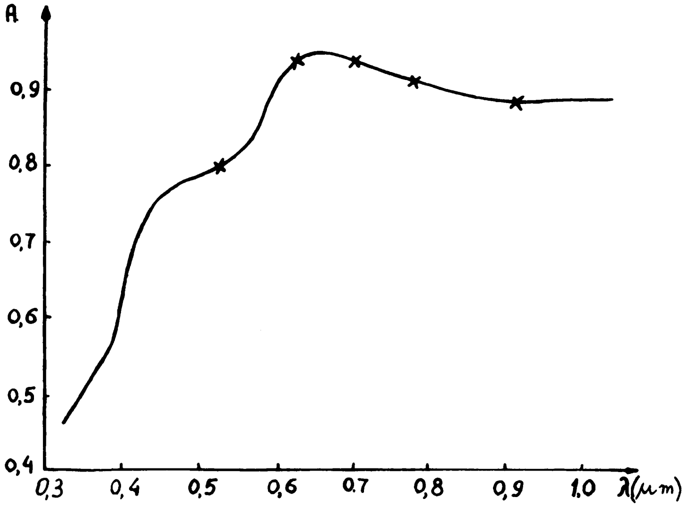

Fig. 1. The measured (full line) and the calculated (crosses) albedo of Venus for $\tau = 60$.

TABLE I

Wavelength dependence of cloud parameters

λ (μm)	$\tau_{R,\lambda}$	τ_1	$N \times 10^{-8}$ (part cm^{-2})
0.69	7.9	13.0 ± 1.5	1.5
0.86	3.3	8.5 ± 0.5	1.2
1.14	1.1	13.5 ± 0.5	1.0

change significantly with the wavelength. The scattering functions are less elongated than for larger particles. Therefore, the optical thicknesses obtained are smaller, as Table I shows. The last colum in the table gives the number of cloud particles per unit cross section in the whole cloud column,

$$N = \frac{\tau}{K},$$

where K is the scattering cross section.

The spectral dependence of N is weak, which confirms our approach.

2. The Infra-Red Range

The difficulty in modelling the infra-red reflection spectrum comes from the line structure of the absorption spectra of gases. The concepts of the absorption coefficient and the radiative transfer equation retain their meanings only for monochromatic radiation. Therefore, calculations of the reflection spectrum of Venus include, as a rule, multiple scattering and absorption by cloud particles, but only indirect evaluations of the gas absorption are presented. Such evaluations are insufficient to examine the possibility of water clouds.

We used the approach to study the paths of photons in a scattering medium of van de Hulst, Irvine, Romanova, and the Monte-Carlo technique. The reflected flux at the upper boundary of the atmosphere is equal to:

$$F_{\Delta\lambda} = \int_0^\infty J_{\Delta\lambda}(l)\, P_{\Delta\lambda}\left[M_{\Delta\lambda} + \varrho_{cl} l\right] \exp\left[-\alpha_{\Delta\lambda} l\right] \mathrm{d}l .$$

Here $J_{\Delta\lambda}$ is the distribution of paths l of photons for pure scattering of the reflected light. This function was calculated by the Monte-Carlo method. $P_{\Delta\lambda}(M)$ is the transmission function for CO_2. Experimental data for $\Delta\nu = 25\ \mathrm{cm}^{-1}$ were used. $M_{\Delta\lambda}$ is the gas mass along the slant path above the cloud:

$$M_{\Delta\lambda} = (\sec\zeta + \sec\bar{\zeta}) \int_{z_2}^\infty \varrho(z) \left(\frac{p(z)}{p_0}\right)^{n_{\Delta\lambda}} \mathrm{d}z ,$$

where z_2 is the upper boundary of the cloud; p, the pressure, $p_0 = 1$ atm; ζ, the zenith distance of the Sun; $\bar{\zeta}$, the mean zenith angle of propagation of the reflected light above the cloud; ϱ_{cl} is the mean density of CO_2 within the cloud, or in the upper part of the cloud; $\alpha_{\Delta\lambda}$, the spectral absorption coefficient of cloud particles.

An ice cloud model was considered. In Figures 2 and 3 models of ice clouds ($n = 1.33$; $r = 1.1\ \mu$m) are given, without (Figure 2) and with (Figure 3) absorption by CO_2 molecules. In both cases $M = 0$, i.e. the absorption above the cloud is neglected.

The spectral geometric albedo is considered relative to its value at $\lambda = 1.85\ \mu$m. The

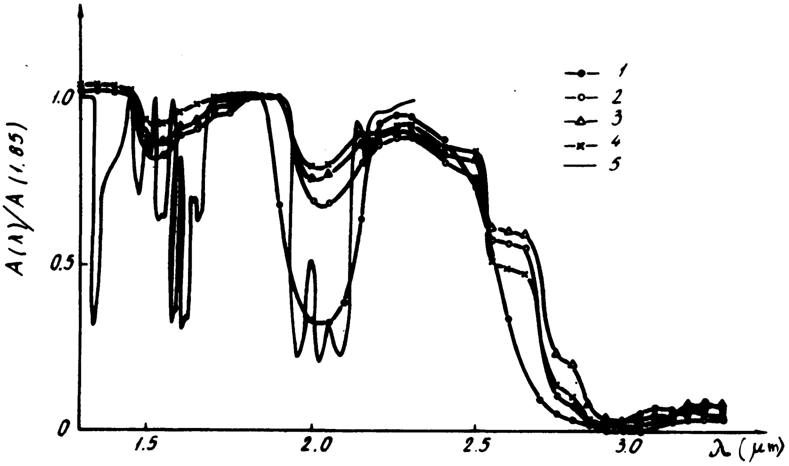

Fig. 2. The spectral albedo without CO_2 absorption. Curves 1 and 5 – the averaged data of Kuiper and Bottema; 2 – calculations for $\zeta = 45°$, $\tau = 20$; 3 – ditto but $\zeta = 70°$; 4 – ditto but $\zeta = 45°$, $\tau = 10$.

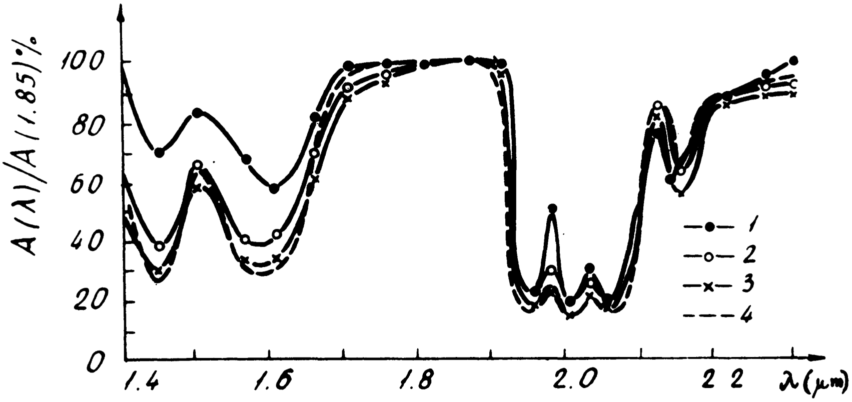

Fig. 3. The spectral albedo with CO_2 absorption. Curves: 1 – experimental data as in Figure 2; 2 – calculations for $\zeta = 70°$; $\tau = 20$; 3 – ditto but $\zeta = 45°$; 4 – ditto but $\zeta = 10°$.

thick line is the averaged experimental data of Kuiper (at $\lambda \leqslant 1.8$ μm) and Bottema (at $\lambda > 1.8$ μm). The figures show that the ice absorption is small compared to CO_2 absorption. So the suggestion of an ice cloud may not contradict the reflection spectrum.

The optical depth of the cloud was varied in the range 10–20 with little influence on the reflection. It is still less influenced by the medium under the cloud. The figures show the effect of the zenith distance of the Sun – the bands become deeper as the Sun rises. In Figure 4 the calculations are compared with the corresponding experimental data and the fine spectral structure is shown. Figure 5 gives the results of calculations

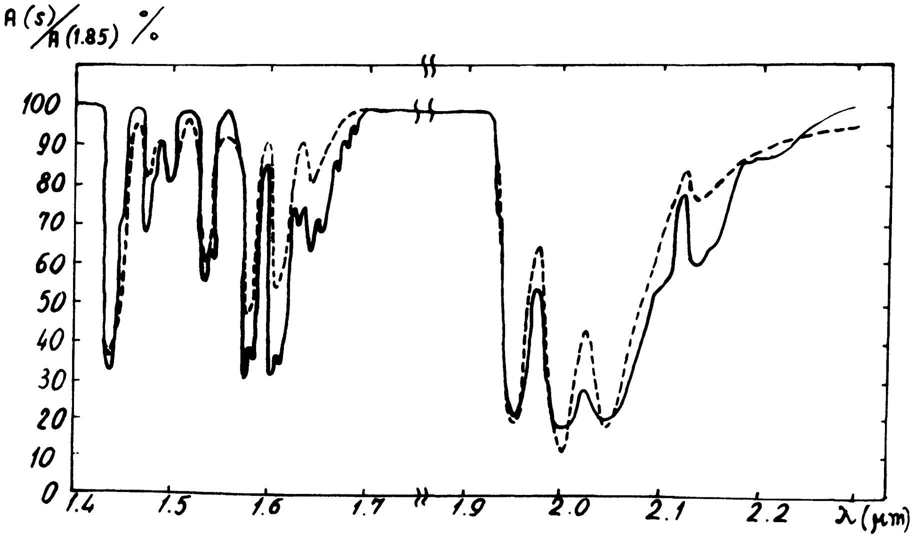

Fig. 4. The reflection spectrum with fine spectral structure. Full line – measurements; dashed line – calculations.

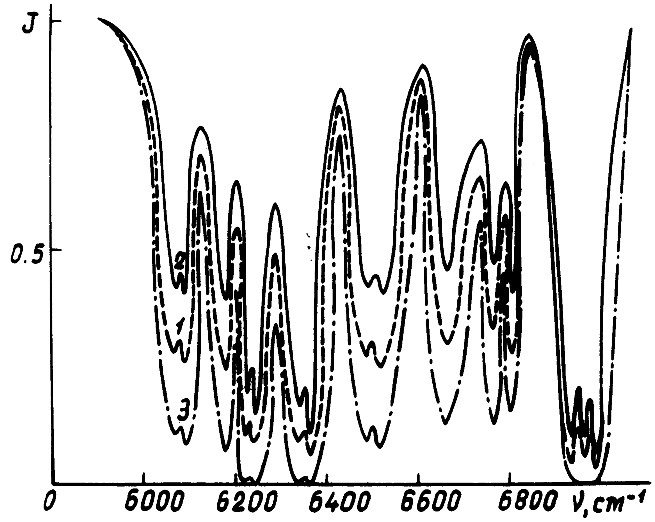

Fig. 5. The calculated reflection spectrum for $\alpha = 67°$. Curves 1 and 2: two cloud layers with upper boundaries at $z_1 = 70$ km and $z_2 = 72$, curve 1 : $\tau^* = 1$, curve 2 : $\tau^* = 2$, curve 3 : only the lower cloud.

for two-layer cloud models. The absorption of CO_2 above and between the clouds is also taken into account. The calculations were made for a phase angle α of 67°.

3. Conclusions

The following conclusions were drawn from the consideration of the two cloud layers:

The addition of a thin upper cloud leads to a decrease of the band equivalent widths, compared with the case of one lower cloud. The intensity of the reflected radiation is very sensitive to the small optical thickness τ^* of the upper cloud. The sensitivity is especially significant for strong bands.

The explanation of the phenomena described is that the number of photons reflected from the upper cloud increases with τ^*, and for these photons the abundance of CO_2 along the path is small.

In dealing with Venus we have to remember that there may be several cloud layers, and the situation is much more complicated than is usually considered in the spectroscopic evaluations of the water vapour abundance.

The optical thickness of the lower cloud is 30, its upper boundary at $z_1 = 70$ km. The lower cloud is in the layer 71–72 km, its optical thickness is 1 or 3.